# Dynamic profilometry without out-of-plane conversion to measure vibration frequency of a cantilever beam



2009 J. Opt. A: Pure Appl. Opt. 11 085409

(http://iopscience.iop.org/1464-4258/11/8/085409)

J. Opt. A: Pure Appl. Opt. **11** (2009) 085409 (7pp) doi:10.1088/1464-4258/11/8/085409

# Dynamic profilometry without out-of-plane conversion to measure vibration frequency of a cantilever beam

**C Meneses-Fabian[1], G Rodriguez-Zurita[1], R Rodriguez-Vera[2], F Mendoza-Santoyo[2] and Amalia Martinez[2]**

[1] Benemérita Universidad Autónoma de Puebla, Facultad de Ciencias Físico-Matemáticas, Avenida San Claudio y 18 Sur, C U San Manuel, Puebla, PUE 72570, Mexico
[2] Centro de Investigaciones en Optica A C, Loma del Bosque No. 115, Lomas del Campestre, León, GTO 37150, Mexico

E-mail: cmeneses@fcfm.buap.mx

Received 5 January 2009, accepted for publication 20 May 2009
Published 6 July 2009
Online at stacks.iop.org/JOptA/11/085409

**Abstract**
A new technique to measure oscillation frequencies and modal shapes of an Euler–Bernoulli cantilever beam using dynamic profilometry and phase extraction techniques is presented. The proposed technique does not require a fixed reference or out-of-plane conversion, and works on nonstop vibration. A binary pattern is projected on the cantilever beam surface mechanically forced to vibrate harmonically in a natural mode. The Fourier transform method is employed to obtain the phase difference between two consecutive frames, in particular it is applied to four consecutive frames so that three consecutive phase differences are available. Finally, the three-step temporal phase-shifting technique is applied to measure the vibration's eigenvalues and eigenfunctions. This paper presents the analysis of the underlying theory and the experimental results obtained.

**Keywords:** interference, phase retrieval, gratings, vibrations and mechanical waves

(Some figures in this article are in colour only in the electronic version)

## 1. Introduction

The study of vibrations on a cantilever beam is a formidable task and over many years has been investigated by many scientists and engineers. Some researchers have mathematically modeled a number of configurations [1–8] for different boundary conditions [9]. Others have directed their efforts to avoiding, suppressing and controlling vibrations [10–13]. Some others have developed and implemented numerous techniques to measure these vibrations. Some techniques use accelerometers to measure elasticity moduli and oscillation frequencies in wood cantilevers [14], in depth cracks [5, 15] and in vibration analysis on a metallic plate by using laser vibrometers [16]. Also a Bragg grating fiber sensor has been used [17] to measure displacements with high precision by measuring changes in the wavelength of the light conveyed through the fiber. But some of these techniques are intrusive, i.e. need contact, or are applied point by point on the object. Non-intrusive measurements and non-contact ones with low spatial resolution have been realized by capacitive [18] and inductive [19] transducers based on electromagnetic principles. In order to overcome these drawbacks, many optical non-intrusive, non-contact and non-destructive techniques have been proposed to measure vibration frequency and modal shape indirectly, including holographic interferometry [20, 21], laser Doppler velocimetry [22–24], stroboscopic heterodyne holographic interferometry [25], electronic speckle pattern interferometry [26–28], Moiré fringe projection [29, 30], shadow Moiré [31, 32] and fringe projection profilometry [33–35]. Direct measurement can also be carried out by optical deflectometry [36–39] or by using oblique ray techniques [40] based principally in optical triangulation [41–44]. With optical beam deflectometry, Jenkins *et al* [38] have obtained measurements of the vibration frequencies from a cantilever beam with a maximum per cent deviation calculated of approximately 8.8%. All the aforementioned techniques need a fixed reference to obtain modal shapes from a cantilever beam. Sometimes, the reference is the same object in its stationary state while in others it is a flat surface generally next to the object. Therefore, in many cases, two frames are needed and the target is necessarily halted. However, recently, capturing both reference and object information in a single frame has been proposed: the vibration amplitude measurement was carried out by using a structured light pattern from a four-core optical fiber [45] with no need to bring the object to a halt. Also, four phase-shifted interferograms may be captured in a single frame to measure the amplitude of a vibrating disc [46]. Although these last techniques have many advantages, they all use a fixed reference. More recently, a technique to measure natural modal shapes from a cantilever beam which uses a variable reference and two frames but without having the requirement to stop the vibration was proposed [47]. In this paper fringe projection profilometry and Fourier transform profilometry using a variable reference are used to measure the oscillation frequency on an Euler–Bernoulli cantilever beam vibrating in a natural mode, where low frequencies, less than 200 Hz, and large amplitudes in the range from 0.1 to 100 mm peak-to-peak are considered. The reference is the frame before the current frame, wherewith the phase differences from two consecutive frames is obtained and an approximation of the natural modal shape is measured. It is worth mentioning here that, to obtain the exact modal shape, an out-of-plane conversion [48] must be applied, but this task is not simple and often only an approximation is available, and the measurement is obtained with an error. With four consecutive frames, three consecutive phase differences can be obtained and a $3 \times 3$ system of equations is defined. This system is interpreted as a three-step temporal phase-shifting technique. In addition, this proposed technique is applied without out-of-plane conversion, and by resolving the $3 \times 3$ system the oscillation frequency can be determined for the six first modes. The analysis of the underlying theory and the experimental results obtained are presented.

## 2. Static projected fringe profilometry

Projected fringe profilometry [49–51] is today one of the most used techniques to measure the depth or shape of 3D objects. It has been applied in diverse fields, including the manufacturing industry, as a quality inspection technique, monitoring of products, inverse engineering, biomedical engineering, orthopedics and surgery, computer graphics and vision, and optical surface evaluation. The technique consists of quantifying in-plane displacements by phase extraction methods [52, 53] from a point in the projected pattern on the object surface with respect to a point on a fixed reference surface, converting this point-to-point comparison to out-of-plane values [48].

In order to apply Fourier transform profilometry, the projected grating of period $p = 1/\mu_0$ is modeled by a two-beam interference pattern [47], namely

$$I(x, y) = a(x, y) + b(x, y)\cos[2\pi\mu_0 x + \phi(x, y)], \quad (1)$$

where $a(x, y)$ is interpreted as the background intensity, $b(x, y)$ is the modulation intensity, $\mu_0$ is the spatial carrier frequency in the $x$ direction and $\phi(x, y)$ is the phase contribution introduced by the object surface profile.

The phase $\phi(x, y)$ is calculated with phase extraction techniques and the object surface profile can be obtained by an out-of-plane conversion [48]. The height of the object is represented as a scalar function of two variables, which can be generally written as

$$z(x, y) = \Gamma(x, y, p, \alpha, \beta) \cdot \phi(x, y), \quad (2)$$

where a linear relationship between the measured phase and the out-of-plane values via a function gamma $\Gamma$ is assumed.

## 3. Dynamic Fourier transform profilometry

The term ‘dynamic profilometry’ refers to the static profilometry principle with a variable reference. In this paper we propose a new technique to study vibration modes on a homogeneous clamped–free cantilever beam. The experimental set-up used is depicted in figure 1(a), where the cantilever beam is forced to vibrate in one of its natural modes. Both the angles $\alpha$ and $\beta$ are formed by the Ronchi grating projector and by the observing CCD camera with respect to the cantilever beam surface normal, respectively. The projector images a Ronchi grating on the cantilever beam surface and a CCD camera captures the deformed pattern. Figure 1(b) shows the cantilever beam vibrating at its first natural mode. The top image shows a top view, while the bottom image shows a side view depicting the deformed fringes due to vibration. The cantilever beam amplitude variations are now time-, $t$, dependent and therefore equations (1) and (2) are accordingly time-dependent:

$$I_n(x, y, t) = a(x, y) + b(x, y)\cos[2\pi\mu_0 x + \phi_n(x, y, t)], \quad (3)$$

$$z_n(x, y, t) = \Gamma(x, y, p, \alpha, \beta) \cdot \phi_n(x, y, t), \quad (4)$$

where $n$ indicates the cantilever beam natural mode number. $\phi_n(x, y, t)$ depends also on $n$, varying harmonically in space and time, and directly proportional to the fringe displacement: its value increases as the vibration amplitude increases, and decreases to zero when it is at a stationary state or at an equilibrium position. In equation (4), we have assumed that the function $\Gamma$ depends neither on time nor on $n$.

For $t = t_k$, if we define $I_n(x, y, t_k) = I_{n,k}(x, y)$ and $\phi_n(x, y, t_k) = \phi_{n,k}(x, y)$, equation (3) can be expressed as

$$I_{n,k}(x, y) = a(x, y) + b(x, y)\cos[2\pi\mu_0 x + \phi_{n,k}(x, y)], \quad (5)$$

where the functions $a(x, y)$ and $b(x, y)$ are considered time-independent and subscript $k$ is a positive integer corresponding to the $k$th CCD captured pattern $I_{n,k}(x, y)$. It is assumed that the integration time $\tau_i$ of the CCD camera is smaller than the period $\tau_c$ of the captured pattern, i.e. $\tau_i \ll \tau_c$, thus avoiding the zero-order Bessel function that would then characterize the captured pattern [54–57]. Now, applying the Fourier transform method, equation (5) can be rewritten as

$$I_{n,k}(x, y) = a(x, y) + d_{n,k}(x, y) + d^*_{n,k}(x, y), \quad (6)$$

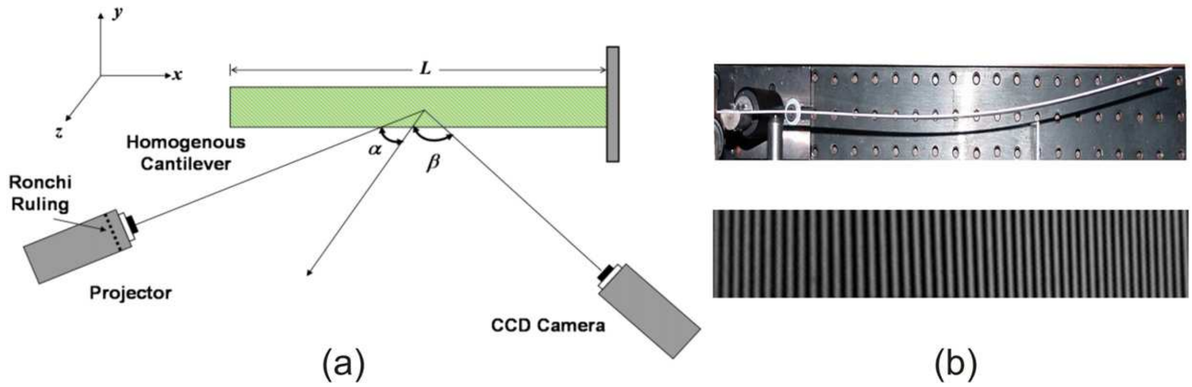


**Figure 1.** (a) Experimental set-up. A Ronchi grating is projected onto a homogeneous clamped–free cantilevered beam and the image is captured by a CCD camera. Projector and CDD form angles $\alpha$ and $\beta$ with respect to the normal line to the cantilever, respectively. (b) Cantilever beam vibrating at mode 1: top image is a top view and bottom image is a side view.

where the asterisk denotes the complex conjugate of $d_{n,k}(x, y)$, which is given by

$$d_{n,k}(x, y) = \tfrac{1}{2}b(x, y)\exp\{\mathrm{i}[2\pi\mu_0 x + \phi_{n,k}(x, y)]\}. \quad (7)$$

As is well known, equation (7) can be obtained from equation (6) by applying the Fourier transform method to extract the phase, introduced by Takeda *et al* [58] and later studied by many other researchers [59–64]. Hence

$$d_{n,k}(x, y) = \Im^{-1}\{\Im\{I_{n,k}(x, y)\} \cdot w(\mu, \nu)\}, \quad (8)$$

where $\Im$ is the Fourier transform operator and $w(\mu, \nu)$ is the window function, which is used as a filter in the frequency space to pass through only one lobe of the Fourier spectrum. The filtering offers the unique advantage to eliminate the possible ambiguity to allocate the filtered component to the center of coordinates, a feature required in order to miss the carrier frequency in the typical Fourier transform method [58].

Then, applying the Fourier transform method for two consecutive patterns at instants $t_k$ and $t_{k+1}$ ($k$ and $k+1$ frames), it is possible to calculate the phase difference by performing the following calculation:

$$\Delta\phi_{n,k}(x, y) = \phi_{n,k+1}(x, y) - \phi_{n,k}(x, y) = \frac{d_{n,k+1}(x, y)}{d_{n,k}(x, y)}. \quad (9)$$

With this procedure, we have eliminated the modulation intensity $b(x, y)$ and the linear phase $2\pi\mu_0 x$, and therefore the carrier frequency $\mu_0$. Note that, in this new technique, the reference surface and the period of the Ronchi grating are unknown, not needed, parameters. This constitutes an enormous advantage since now we do not have to calculate the way in which the projected pattern on the reference surface becomes deformed [47], a variable eliminated when dividing $d_{n,k+1}$ by $d_{n,k}$, in order to quantify the cantilever beam modal shapes. Another outstanding advantage is that problems like CCD detector nonlinearity and non-uniform illumination become eliminated [59, 65]. Furthermore, if certain experimental conditions that involve adjustment of variables such as the Ronchi grating period, the CCD camera capture time, the angles $\alpha$ and $\beta$, and the vibration amplitude can be chosen to fulfill that $\Delta\phi_{n,k}(x, y) \leqslant 2\pi$, there will be no need to phase-unwrap the data.

Observe that, if the $\Gamma$ function was a constant [47], equation (9) would express the modal shape of the cantilever beam. But, when $\Gamma$ cannot be considered as a constant, equation (9) would only give an approximation to the modal shapes. Introducing the $\Gamma$ function in equation (6), it can be written as

$$\begin{aligned}\Delta z_{n,k}(x, y, t) &= z_{n,k+1}(x, y, t) - z_{n,k}(x, y, t)\\ &= \Gamma(x, y, p, \alpha, \beta) \cdot \Delta\phi_{n,k}(x, y).\end{aligned} \quad (10)$$

Equation (10) indicates amplitude differences between times $t_k$ and $t_{k+1}$, and is considered as the exact modal shape expression, which is called dynamic profilometry due to the variable reference.

## 4. Vibration frequency measurement

This section shows the procedure to calculate the vibration frequency from the phase difference measurements, without the need to perform the out-of-plane conversion, avoiding also the need to know the conversion $\Gamma$ function. In order to measure the vibration frequency, we assume the cantilever beam vibrating in one of its natural frequencies such that the amplitude at point $(x, y)$ varies according to the Euler–Bernoulli solution [1, 9]:

$$z_n(x, y, t) = A_n(x, y)\sin(\omega_n t + \varphi_0), \quad (11)$$

where $A_n$ is the maximum amplitude, $\omega_n$ is the oscillation temporal frequency and $\varphi_0$ is an initial phase. Substituting $t_{k+1} = t_k + \tau_c$ in equation (11), the amplitude differences may be written as

$$\Delta z_{n,k}(x, y) = 2A_n(x, y)\sin(\tfrac{1}{2}\Delta\varphi_n)\cos(\varphi_{n,k} + \tfrac{1}{2}\Delta\varphi_n), \quad (12)$$

where $\Delta\varphi_n = \omega_n\tau_c$ and $\varphi_{n,k} = \omega_n t_k + \varphi_0$. Now combining (10) and (12) the phase differences can be related by

$$\Delta\phi_{n,k}(x, y) = \phi_{An}(x, y)\sin(\tfrac{1}{2}\Delta\varphi_n)\cos(\varphi_{n,k} + \tfrac{1}{2}\Delta\varphi_n), \quad (13)$$

where $\phi_{An}(x, y) = 2A_n(x, y)/\Gamma(x, y, p, \alpha, \beta)$. Equation (13) expresses the relationship between the oscillatory behavior of a cantilever beam based on the Euler–Bernoulli model and the phase differences measured by dynamic profilometry (equation (10)). Now for $q$ consecutive phase differences equation (13) can be generalized to

$$\Delta\phi_{n,k+q}(x, y) = \phi_{An}(x, y) \sin\left(\tfrac{1}{2}\Delta\varphi_n\right) \times \cos[\varphi_{n,k} + \tfrac{1}{2}(2q + 1)\Delta\varphi_n], \tag{14}$$

where $q$ indicates the number of consecutive phase differences from which any number of equations may be obtained. Since equation (14) has only three unknowns, $\phi_{An}$, $\Delta\varphi_n$ and $\varphi_{n,k}$, only three values of $q$ are needed in order to solve for three unknowns. For example, for $q = 0, 1, 2$ the equations, $\Delta\phi_{n,k}$, $\Delta\phi_{n,k+1}$ and $\Delta\phi_{n,k+2}$ are obtained and a $3\times3$ system is formed, which mathematically can be solved to obtain

$$\cos(\Delta\varphi_n) = \frac{\Delta\phi_{n,k}(x, y) + \Delta\phi_{n,k+2}(x, y)}{2\Delta\phi_{n,k+1}(x, y)}, \tag{15}$$

Solving for $\Delta\varphi_n$ and using the definition $\Delta\varphi_n = \omega_n\tau_c$, the temporal frequency can be calculated by means of

$$\omega_n = \frac{1}{\tau_c} \cos^{-1}\left[\frac{\Delta\phi_{n,k}(x, y) + \Delta\phi_{n,k+2}(x, y)}{2\Delta\phi_{n,k+1}(x, y)}\right], \tag{16}$$

where we have assumed that the capture time $\tau_c$ is known and remains constant. Thus, out-of-plane conversion is avoided. Equation (16) is the expression that allows us to know the oscillation frequency in a homogeneous cantilever beam vibrating in a natural mode by applying dynamic profilometry with four consecutive frames. Note that $\omega_n$ is a function of the phase differences and the capture time $\tau_c$, which has been calculated solely with three values of $q$.

## 5. Experimental results

The experimental set-up is that in figure 1(a), a clamped–free cantilever beam made of plastic, $300 \times 40 \times 1$ mm$^3$ in size, was arranged to be mechanically excited near its clamped end with a small pin on the center of a loudspeaker connected to a signal generator. An angle $\alpha = 47°$ for a 5 mm fringe period projected on the cantilever beam surface is formed by the projector. A CCD camera capturing 402 frames per second, which is $\tau_c = 1/402 \approx 2.49 \times 10^{-3}$ s, is set perpendicular to the cantilever surface forming an angle $\beta = 0°$. The CCD camera, PixeLINK PL-B741F, is configured to integrate an image in a time $\tau_i = 1/8000 = 0.125 \times 10^{-3}$ s, securing the condition $\tau_i \ll \tau_c$ is fulfilled and equation (7) is validated.

Adjusting the signal generator to a resonant frequency, the cantilever beam is forced to oscillate harmonically in a natural mode. The frequency is measured with an oscilloscope and is stored for further comparison. The CCD camera captures and digitizes four consecutive fringe patterns of 64 pixels $\times$ 640 pixels resolution, with 256 gray levels. The resulting patterns are stored in a PC memory. In order to show how this technique is set to work, let us process a captured pattern $I_{1,k}$ for mode 1 (figure 2(a)). The Fourier transform is computed (see figure 2(b)) and filtered in the Fourier space in

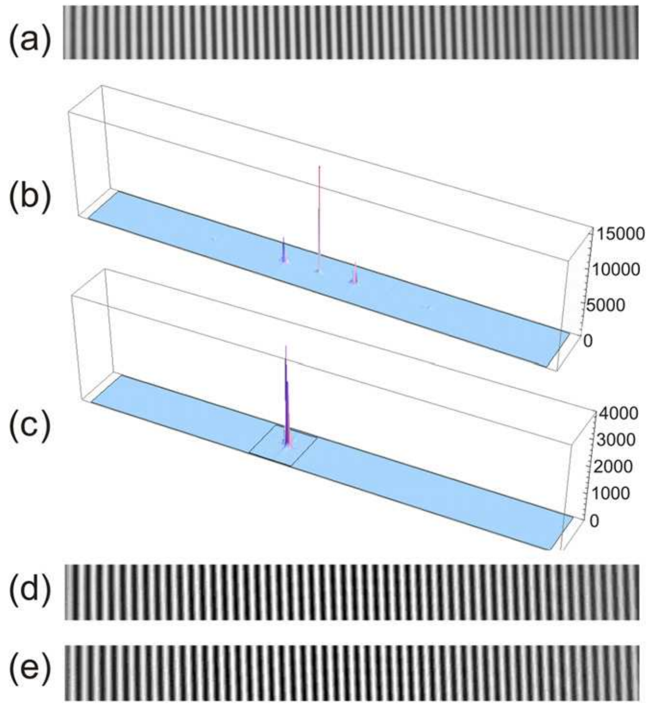


**Figure 2.** Fourier transform method to obtain the $d_k$ term (equation (9)), all images are $64 \times 640$ resolution pixels with 256 gray levels: (a) fringe pattern captured at an instant $t_k$, (b) Fourier transform of the fringe pattern, (c) filtering of the pattern Fourier transform to obtain only one through lobe, (d) real, and (e) imaginary part of $d_k$.

order to obtain only one through lobe (figure 2(c)), then the inverse Fourier transform is computed and the $d_{1,k}$ function is calculated (equation (9)). Figures 2(d) and (e) show the real and imaginary part, respectively, so that phase extraction by the Fourier transform method is performed [58]. Now, for two consecutive patterns $I_{1,k}$ and $I_{1,k+1}$, $d_{1,k}$ and $d_{1,k+1}$ are obtained, and the phase difference $\Delta\phi_{1,k}$ is calculated by equation (13).

Figure 3(a) shows four consecutive patterns for resonant mode 1. Applying the Fourier transform method and consecutive divisions between $d_{1,k+q}$ and $d_{1,k+q}$, as explained above, the phase difference $\Delta\phi_{1,k+q}$ is calculated for $q = 0, 1, 2$ as indicated in relationship (14), with the results shown in figure 3(b) (upper, middle and lower images for $q = 0, 1, 2$, respectively). Each $\Delta\phi_{1,k+q}$ is an equation with three unknowns and, as we have calculated three equations, then we have a $3 \times 3$ system of equations. Equation (15) is experimentally obtained (figure 3(c) top image) and the oscillation frequency is calculated for each point on the cantilever beam using equation (16) (figure 3(c) middle image). By assuming that each point on the cantilever beam surface oscillates at the same frequency, an average over all points may decrease the noise in the measurements and give better results, see figure 3(c) bottom image.

We repeated this procedure for natural modes 2–6. Figure 4(a) shows five fringe patterns captured (the other three patterns for each mode are not shown) for 2–6 modes, respectively. Figure 4(b) shows the phase differences for two

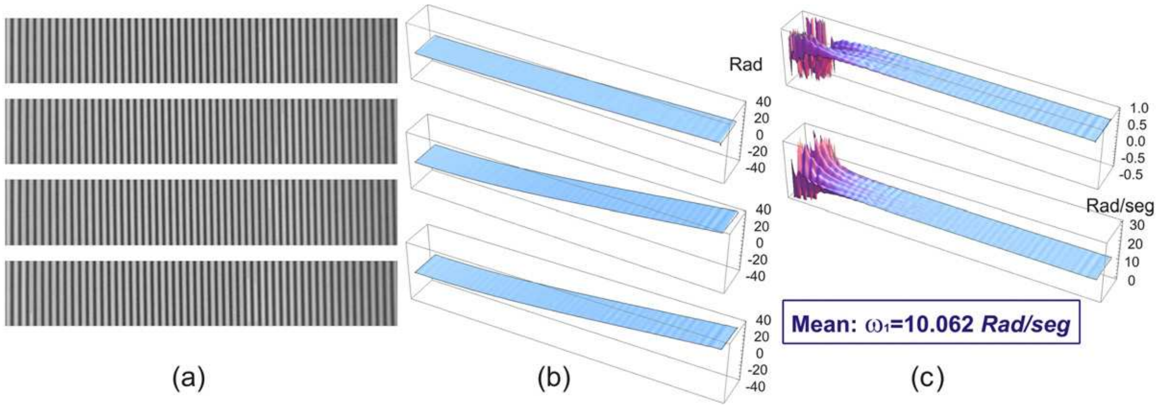


**Figure 3.** Measurement frequency of mode 1, dynamic profilometry by Fourier transform and temporal phase-shifting methods, all images of 64 × 640 resolution pixels and code at 256 gray levels: (a) four consecutive fringe patterns, (b) consecutive phase differences, (c) top graph is the $\cos(\Delta\varphi_1)$, middle graph is the $\omega_1$ for each point $(x, y)$ and bottom graph is an average.

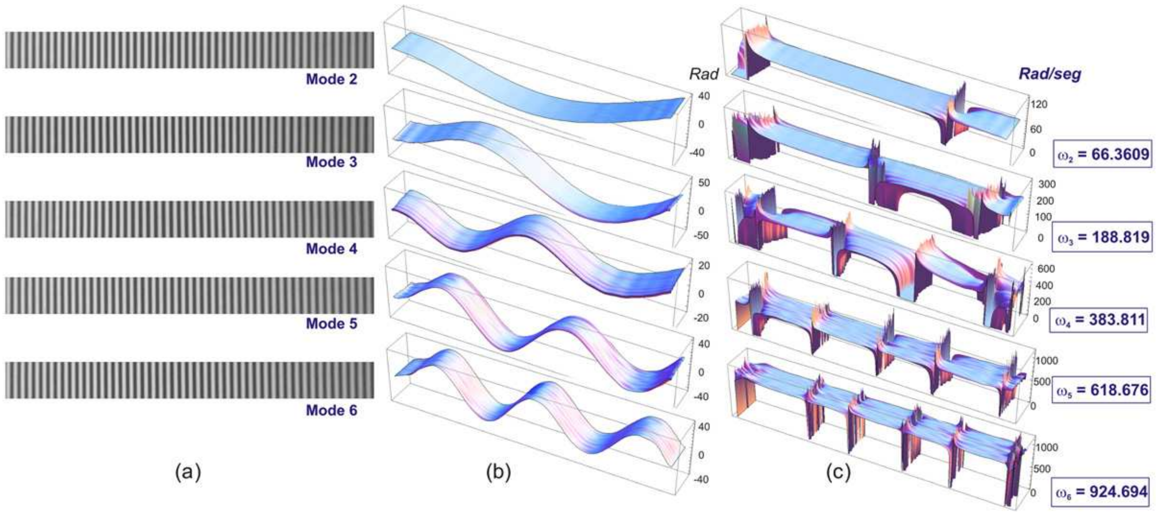


**Figure 4.** Measurement of frequency from modes 2–6 by dynamic interferometric profilometry, all images of 64 × 640 resolution pixels with 256 gray levels: (a) fringe patterns, (b) phase differences, (c) $\omega_1$, both for each point $(x, y)$, and the computed average.

consecutive frames (the other two phase differences for each mode are not shown) and figure 4(c) shows the measurement vibration frequencies, both for each point and an average on the cantilever beam, where the average is obtained for all points except where the value is not defined, where there is a node, due to a division by zero in equation (16).

Table 1 shows the signal generator forced frequency as measured with the oscilloscope, the vibration frequency measured with dynamic interferometric profilometry and an estimation of the per cent deviation in the measurement for modes 1–6. The small deviation in the forced frequency column, column 2, is due to normal noise fluctuations in the oscilloscope. It can be seen that the vibration frequency measured by dynamic interferometric profilometry is very close to the frequency data measured with the oscilloscope. The last column shows the per cent deviation between the ranged oscilloscope measurements and column 3. Note that the largest per cent deviations are no greater than 2.63%, or the error is no greater than 1.2 Hz, and the minimum per cent deviation is 0.004%, or 0.0014 Hz. In table 1, the deviations in the measurements can happen due to the sampling of the data in the vicinity of a maximum or a minimum of the vibration, which increases as the vibration frequency approaches the sampling limit imposed by the data capture frequency. The applied phase extraction method can also contribute to some error, in particular, if the Fourier transform method is used for spatial filtering in the frequency domain of the interference pattern to position the desired lobe at the origin. A small linear phase can be added to compensate for this deviation from the origin.

## 6. Comments and conclusions

In this paper, the main goal was to prove the viability of our technique. However, we believe it would be worth inspecting further the problem of the vibrations on a cantilever beam in order to study limits and useful approximations in connection to the proposed technique. Related to the former, the maximum measured frequency is imposed by the sampling theorem (Nyquist) which says that such a frequency has to be

**Table 1.** Comparison between the forced frequencies applied to a cantilever beam as measured with an oscilloscope and dynamic interferometric profilometry. Frequencies have units of rad Hz.

| Natural mode $n$ | Forced frequency $\omega_f$ (rad Hz) | Vibration frequency $\omega_n$ (rad Hz) | Per cent deviation (%) $\frac{\omega_f-\omega_n}{\omega_f}\times 100$ | |
|---|---|---|---|---|
| 1 | 10.072–10.135 | 10.062 | 0.10 | 0.72 |
| 2 | 65.471–65.534 | 66.361 | −1.36 | −1.26 |
| 3 | 187.867–188.81 | 188.819 | −0.51 | −0.01 |
| 4 | 373.975–376.237 | 383.811 | −2.63 | −2.01 |
| 5 | 616.003–621.47 | 618.676 | −0.43 | 0.45 |
| 6 | 926.770–936.195 | 924.694 | 0.22 | 1.23 |

half of the data capture frequency. In the present work, the employed camera captures 402 images $s^{-1}$, so 201 Hz is the maximum frequency measurable, that is, $\omega_{max} = 1263$ rad Hz approximately. The minimum frequency could be considered theoretically zero, a situation where the target is found at rest. In this case, the system can be adapted to operate as an optical profilometer. However, in practice, one of the more important restrictions is the spatial resolution of the detector and gray level coding in a pixel.

Using projected fringe profilometry, Fourier transform profilometry and phase extraction techniques that include temporal phase shifting, and without the need for a fixed reference and an out-of-plane conversion, we have demonstrated theoretically and experimentally that it is possible to measure vibration frequencies and modal shapes (eigenvalues and eigenfunctions) on a cantilever beam vibrating forcedly in its natural modes. Note that the measurement made with our technique is more accurate as the maximum per cent deviation from the new technique is only 2.63% as compared to 8.8% as reported by Jenkins *et al* [38]. The accuracy of the new technique can be further improved. Furthermore, these measurements have been made with high precision, and with capturing only four consecutive frames and without having to stop the oscillation. Phase difference was approximated to the modal shape of a cantilever beam, so temporal phase shifting was used to generate a $3 \times 3$ system with their solution giving the oscillation frequency. In addition, we have introduced a new noncontact, non-invasive and non-intrusive technique to measure modal parameters using profilometry in a moving object. We will shortly report on work that we are currently conducting on the forced response on a cantilever beam vibrating in various natural modes simultaneously.

## Acknowledgments

This work was partially supported by the Vice-president of Research and Postgraduate Studies of Benemerita Universidad Autonoma de Puebla (VIEP-BUAP, México) under grant 13/EXC/07 and by the Improvement Program for Young Scientists under grant PROMEP/103.5/07/2594.

## References

[1] Inman D J 2008 *Engineering Vibration* New Jersey, chapter 6, pp 464–531

[2] Gorman D l G, Trendafilova I, Mulholland A J and Horáček J 2007 Analytical modeling and extraction of the modal behavior of a cantilever beam in fluid interaction *J. Sound Vib.* **308** 231

[3] Ciancio P M, Rossit C A and Laura P A A 2007 Approximate study of the free vibrations of a cantilever anisotropic plate carrying a concentrated mass *J. Sound Vib.* **302** 621

[4] Fotouhi R 2007 Dynamic analysis of very flexible beams *J. Sound Vib.* **305** 521

[5] Lam H F, Ng C T and Veidt M 2007 Experimental characterization of multiple cracks in a cantilever beam utilizing transient vibration data following a probabilistic approach *J. Sound Vib.* **305** 34

[6] Magrab E B 2007 Natural frequencies and mode shapes of Timoshenko beams with attachments *J. Vib. Control* **13** 905

[7] Radhakrishnan V M 2004 Response of a cracked cantilever beam to free and forced vibrations *Def. Sci. J.* **54** 31

[8] Wanga J and Qiao P 2007 Vibration of beams with arbitrary discontinuities and boundary conditions *J. Sound Vib.* **308** 12

[9] Leissa A W and Sonalla M I 1991 Vibrations of cantilever beams with various initial conditions *J. Sound Vib.* **150** 83

[10] Librescu L and Na S 1998 Bending vibration control of cantilevers via boundary moment and combined feedback control laws *J. Vib. Control* **4** 733

[11] Guo-Ping C and Yang S X 2006 A discrete optimal control method for a flexible cantilever beam with time delay *J. Vib. Control* **12** 509

[12] Tjahyadi H, He F and Sammut K 2006 Multi-mode vibration control of a flexible cantilever beam using adaptive resonant control *Smart Mater. Struct.* **15** 270

[13] Joshi A 2004 Theoretical and experimental studies on vibration control in cantilever beams using DC magnets *J. Vib. Control* **10** 995

[14] Turk C, Hunt J F and Marr D J 2008 Cantilever-beam dynamic modulus for wood composite products: part 1 apparatus *Research Note FPL-RN-0308* (Madison, WI: US Department of Agriculture, Forest Service, Forest Products Laboratory) p 5

[15] Ngoi B K A, Venkatakrishnan K, Tan B, Nöel N, Shen Z W and Chin C S 2000 Two-axis-scanning laser Doppler vibrometer for microstructure *Opt. Commun.* **182** 175

[16] Moreno D, Barrientos B, Perez-Lopez C and Mendoza-Santoyo F 2005 Modal vibration analysis of a metal plate by using a laser vibrometer and the POD method *J. Opt. A: Pure Appl. Opt.* **7** S356

[17] Dong X, Liu Y, Liu Z and Dong X 2001 Simultaneous displacement and temperature measurement with cantilever-based fiber Bragg grating sensor *Opt. Commun* **192** 213

[18] Goddenhenrich T, Lemke H, Hartmann U and Heiden C 1990 Force microscope with capacitive displacement detection *J. Vac. Sci. Technol.* A **8** 383

[19] Smith J D 1989 *Vibration Measurement and Analysis* (Oxford: Butterworths–Heinemann)

[20] Hazil C R and Mitchell A K 1992 Separation of closely spaced vibration modes using holographic interferometry *J. Sound Vib.* **152** 125
[21] Picart P, Leval J, Pascal J C, Boileau J P, Grill M, Breteau J M, Gautier B and Gillet S 2005 2D full field vibration analysis with multiplexed digital holograms *Opt. Express* **13** 8882
[22] Arruda J R F 1993 Spatial domain modal analysis of lightly-damped structures using holographic interferometry *J. Vib. Acoust.* **115** 225
[23] Lee K M and Polycapou A A 2002 Dynamic microwaviness measurements of supersmooth disk media used in magnetic hard disk drives *Proc. SPIE* **4827** 493
[24] Rothberg S J and Bell J 2000 Guide to translational and rotational vibration measurements on rotors using laser vibrometry *Proc. SPIE* **4072** 210
[25] Brown G C and Pryputniewicz R J 1992 Investigation of submillimeter components by heterodyne holographic interferometry: techniques and analysis *Proc. SPIE* **1755** 120
[26] Høgmoen K and Løkberg O J 1977 Detection and measurement of small vibrations using electronic speckle pattern interferometry *Appl. Opt.* **16** 1869
[27] Tiziani H J and Klenk J 1981 Vibration analysis by speckle techniques in real time *Appl. Opt.* **20** 1467
[28] Mendoza-Santoyo F, Shellabear M C and Tyrer J R 1991 Whole field in-plane vibration analysis using pulsed phase-stepped ESPI *Appl. Opt.* **30** 717
[29] Harding K G and Harris S J 1983 Projection moire interferometer for vibration analysis *Appl. Opt.* **22** 856
[30] Hopstone P, Katz A and Politch J 1989 Infrastructure of time-averaged projection moiré fringes in vibration analysis *Appl. Opt.* **28** 5305
[31] Tay C J, Quan C, Fu Y and Huang Y 2004 Instantaneous velocity displacement and contour measurement by use of shadow moiré and temporal wavelet analysis *Appl. Opt.* **43** 4164
[32] Hung Y Y, Liang C Y, Hovanesian J D and Durelli A J 1977 Time-averaged shadow-moiré method for studying vibrations *Appl. Opt.* **16** 1717
[33] Vest C M and Sweeney D W 1972 Measurement of vibrational amplitude by modulation of projected fringes *Appl. Opt.* **11** 449
[34] Rosvold G O 1994 Video-based vibration analysis using projected fringes *Appl. Opt.* **33** 775
[35] Andrew K M 2005 Optical modal analysis using white-light projected fringes *Soc. Exp. Mech.* **45** 250
[36] Benedetto G, Gavioso R and Spagnolo R 1995 Measurement of microphone membrane displacement with an optical beam deflection technique *Rev. Sci. Instrum.* **66** 5563
[37] Alexander S, Hellemans L, Marti O, Schneir J, Elings V, Hansma P K, Longmire M and Gurley J 1989 An atomic-resolution atomic force microscope implemented using an optical lever *J. Appl. Phys.* **65** 164
[38] Jenkins D F L, Cunningham M J, Clegg W W and Bakush M M 1995 Measurement of the modal shapes of inhomogeneous cantilevers using optical beam deflection *Meas. Sci. Technol.* **6** 160
[39] Putman C A J, Grooth B G, Van Hulst N F and Greve J 1992 A theoretical comparison between interferometric and optical beam deflection lor the measurement of cantilever displacement *AFM Ultramicrosc.* **42–44** 1509
[40] Park D J, Park G J, Aum T S, Yi J H and Kwon J H 2006 Measurement of displacement and vibration by using the oblique ray method *Appl. Opt.* **45** 3732
[41] Clark R R 2003 Triangulation displacement sensor *US Patent Specification* 6,624,899
[42] Kim J K, Kim M S, Bae J H, Kwon J H, Lee H B and Jeong S H 2000 Gap measurement by position-sensitive detectors *Appl. Opt.* **39** 2584
[43] Kim S H, Kim K C and Oh S B 2002 Optical triangulation displacement sensor using a diffractive grating *US Patent Specification* 6,433,857
[44] Kim K C, Oh S B, Kim S H and Kwak Y K 2001 Design of a signal processing algorithm for error minimized optical triangulation displacement sensors *Meas. Sci. Technol.* **12** 1683
[45] Tunç Y S, Özuğurel U D, Karahan B and Naci Inci M 2005 Vibration amplitude analysis with a single frame using a structured light pattern of a four-core optical fibre *Opt. Commun.* **249** 515
[46] Wyant J C 2004 Vibration insensitive interferometric optical testing *Frontiers in Optics, OSA Technical Digest (CD)* paper OTuB2
[47] Meneses-Fabian C, Rodriguez-Vera R, Rayas J A, Mendoza-Santoyo F and Rodriguez-Zurita G 2007 Surface contour from a low-frequency vibrating object using phase differences and the Fourier-transform method *Opt. Commun.* **272** 310
[48] Wang Z, Du H and Bi H 2006 Out-of-plane shape determination in generalized fringe projection profilometry *Opt. Express* **14** 12122
[49] Chen F, Brown G M and Song M 2000 Overview of three-dimensional shape measurement using optical methods *Opt. Eng.* **39** 10
[50] Saldner H O and Huntley J M 1997 Profilometry by temporal phase unwrapping and spatial light modulator based fringe projector *Opt. Eng.* **36** 610
[51] Spagnolo G S, Paoletti D and Ambrosini D 1997 Vibration monitoring by fiber optic fringe projection and Fourier transform analysis *Opt. Commun.* **139** 17
[52] Schwider J 1998 Advanced evaluation techniques in interferometry *Progress in Optics XXVIII* ed E Wolf (Amsterdam: Elsevier) pp 271–359
[53] Malacara D, Servín M and Malacara Z 1998 *Interferogram Analysis for Optical Testing* New York
[54] Hovanesian J D and Hung Y Y 1971 Moiré contour-sum contour-difference, and vibration analysis of arbitrary objects *Appl. Opt.* **10** 2734
[55] Vest C M and Sweeney D W 1972 Measurement of vibrational amplitude by modulation of projected fringes *Appl. Opt.* **11** 449
[56] Chiang F P and Jaisingh G 1973 Dynamic moiré methods for the bending of plates *Exp. Mech.* **13** 168
[57] Ritter R and Meyer H 1980 Vibration analysis of plates by a time-averaged projection-moiré method *Appl. Opt.* **19** 1630
[58] Takeda M, Ina H and Kobayashi S 1982 Fourier-transform method of fringe-pattern analysis for computer-based topography and interferometry *J. Opt. Soc. Am.* **72** 156
[59] Kreis T 1986 Digital holographic interference-phase measurement using the Fourier-transform method *J. Opt. Soc. Am.* A **3** 847
[60] Macy W W Jr 1983 Two-dimensional fringe-pattern analysis *Appl. Opt.* **22** 3898
[61] Bone D J, Bachor H-A and Sandeman R J 1986 Fringe-pattern analysis using a 2D Fourier transform *Appl. Opt.* **25** 1653
[62] Roddier C and Roddier F 1987 Interferogram analysis using Fourier transform techniques *Appl. Opt.* **26** 1668
[63] Onodera R and Ishii Y 1998 Two-wavelength interferometry that uses a Fourier-transform method *Appl. Opt.* **37** 7988
[64] Liu J B and Ronney P D 1997 Modified Fourier transform method for interferogram fringe pattern analysis *Appl. Opt.* **36** 6231
[65] Lovric D, Vucic Z, Gladic J, Demoli N, Mitrovic S and Milas M 2003 Refined fourier-transform method of analysis of full two-dimensional digitized interferograms *Appl. Opt.* **42** 1477